Investigation into the Hydrothermal Assembly of Molybdenum Polyoxoanion Solids in the Presence of 4-Aminobenzoic Acid, Guanidinium Carbonate, and Aminoacetic Acid

Jianjiang Lu and Yan Xu*

School of Science, Nanyang Technological University, Singapore 259756, Republic of Singapore

Received August 3, 1998. Revised Manuscript Received September 23, 1998

The hydrothermal synthesis of three novel molybdenum polyoxoanion solids in the presence of 4-aminobenzoic acid, guanidinium carbonate, and aminoacetic acid and their crystal structures are reported. The layer structure of **1** can be envisioned as bundles of parallel spirals of tetrameric building units connected via shared corners. Pseudo-one-dimensional 4- and 6-ring channels are found in the interlamella region. The chain structure of **2** consists of corner- and edge-sharing MoO_6. Large interstrand separation is created due to the inclusion of $CN_3H_6^+$. The structure of **3** consists of three-dimensional mixed covalent−hydrogen bonded $[(NH_3CH_2COO)_2Mo_8O_{26}]^{4-}$ with large pseudo-one-dimensional channels. Crystal data: $H_8Mo_4N_2O_{13}$ **(1)**, orthorhombic *Pbca*, $a = 7.682(5)$ Å, $b = 15.389(2)$ Å, $c = 18.996(4)$ Å, $V = 2246(2)$ Å^3, $Z = 8$, 1972 reflections, $R_1 = 0.034$ [$I > 2\sigma(I)$]. $CH_{10}Mo_3N_4O_{10}$ **(2)**, monoclinic $P2_1/c$, $a = 7.6158(13)$ Å, $b = 16.5768(11)$ Å, $c = 9.1946(8)$ Å, $\beta = 95.237(8)°$, $V = 1155.9(2)$ Å^3, $Z = 4$, 2020 reflections, $R_1 = 0.0281$ [$I > 2\sigma(I)$]. $C_2H_{15}Mo_4N_3O_{16}$ **(3)**, monoclinic $C2/c$, $a = 17.326(4)$ Å, $b = 10.744(2)$ Å, $c = 18.697(4)$ Å, $\beta = 108.27(3)°$, $V = 3305.0(12)$ Å^3, $Z = 8$, 2896 reflections, $R_1 = 0.0250$ [$I > 2\sigma(I)$].

Introduction

The issue of the assembly of metal oxide based, especially transition metal oxide based, hybrid materials has drawn tremendous attention due to the widespread interest of these materials in contemporary chemical research.[1−5] Many of these hybrid materials are capable of accommodating guest molecules and allowing chemical reactions to take place in the interlamellar region. It is evident that the chemistry of the hybrid materials depends largely on the conditions under which they are crystallized. Although the mechanism by which the hybrid materials are organized remains elusive, what appears to be clear is that chemically robust clusters of polyoxoanions can be assembled through charge-compensating cations, usually organic amines, to form extended structures. While the optimum synthesis conditions leading to desirable products remains debatable, there is an increasing belief in the combined effect of hydrothermal technique and structure-directing agents. This combined effect has been tried out in a variety of organic/transition metal oxide systems, and outcomes appear to be promising. Typical examples which are highly relevant and instructive to our research interests include the cooperative assembly of organic/reduced molybdenum phosphates,[6] organic/vanadium oxides,[7−9] organic/alkali metal molybdenum(VI) (W^{6+}, V^{6+}) organophosphonates,[10,11] and organic/molybdenum(VI) polyoxoanions.[12−15]

The achievement in the assembly of molybdenum(VI) polyoxoanion based phases under hydrothermal condi-

* Current mailing address of corresponding author: Division of Chemistry, School of Science, Nanyang Technological University, 469 Bukit Timah Road, Singapore 259756, Republic of Singapore. E-mail: xuy@nievax.nie.ac.sg.

(1) Whittingham, M. S.; Jacobson, A. J. *Intercalation Chemistry;* Academic Press: New York, 1981.
(2) Cheetham, A. K. *Science* **1994**, *264*, 794 and references therein.
(3) Clearfield, A. *Chem. Rev.* **1988**, *88*, 125.
(4) Cox, P. A. *Transition Metal Oxides;* Clarendon Press: Oxford, England, 1995.
(5) Suib, S. L. *Chem. Rev.* **1993**, *93*, 803.
(6) Haushalter, R. C.; Mundi, L. A. *Chem. Mater.* **1992**, *4*, 31 and references therein.
(7) (a) Huan, G. H.; Jacobson, A. J.; Johnson, J. W.; Corcoran, E. W., Jr. *Chem. Mater.* **1990**, *2*, 2. (b) Johnson, J. W.; Jacobson, A. J.; Butler, W. M.; Rosenthal, S. E.; Brody, J. F.; Lewandowski, J. T. *J. Am. Chem. Soc.* **1989**, *111*, 381. (c) Vaughey, J. T.; Harrison, W. T. A.; Dussack, L. L.; Jacobson, A. *J. Inorg. Chem.* **1995**, *33*, 4307.
(8) (a) Soghomonian, V.; Haushalter, R. C.; Chen, Q.; Zubieta, J. *Science* **1993**, *256*, 1596. (b) Soghomonian, V.; Chen, Q.; Haushalter, R. C.; Zubieta, J.; O'Connor, C. J. *Science* **1993**, *259*, 1956. (c) Bonavia, G., Haushalter, R. C., O'Connor, C. J.; Zubieta, J. *Inorg. Chem.* **1996**, *35*, 5603.
(9) Zhang, Y.; DeBord, J. R. D.; O'Connor, C. J., Haushalter, R. C.; Clearfield, A.; Zubieta, J. *Angew. Chem., Int. Ed. Engl.* **1996**, *35*, 989.
(10) Harrison, W. T. A.; Dussack, L. L.; Jacobson, A. J. *Inorg. Chem.* **1995**, *34*, 4774 and references therein.
(11) (a) Harrison, W. T. A.; Dussack, L. L.; Jacobson, A. J. *Inorg. Chem.* **1994**, *33*, 6043. (b) Harrison, W. T. A.; Dussack, L. L.; Jacobson, A. J. *Inorg. Chem.* **1995**, *34*, 4774. (c) Harrison, W. T. A.; Dussack, L. L.; Jacobson, A. J. *J. Solid. State Chem.* **1995**, *116*, 95. (d) Harrison, W. T. A.; Dussack, L. L.; Vogt, T.; Jacobson, A. J. *J. Solid. State Chem.* **1995**, *120*, 112.
(12) Guo, J. D.; Zavalij, P.; Whittingham, M. S. *Chem. Mater.* **1994**, *6*, 357. (b) Guo, J. D.; Zavalij, P.; Whittingham, M. S. *J. Solid. State Chem.* **1994**, *31*, 833. (c) Guo, J. D.; Zavalij, P.; Whittingham, M. S. *J. Solid. State Chem.* **1995**, *117*, 323.
(13) (a) Khan, M. I.; Chen, Q.; Zubieta, J. *Inorg. Chim. Acta* **1993**, *213*, 325. (b) Zapf, P. J.; Haushalter, R. C.; Zubieta, J. *Chem. Mater.* **1997**, *9*, 2019. (c) Zapf, P. J.; Haushalter, R. C.; Zubieta, J. *Chem. Commun.* **1997**, 321.
(14) Range, K.; Fassler, A. *Acta Crystallogr., Sect. C* **1990**, *46*, 488.

10.1021/cm9805525 CCC: $15.00
Published on Web 11/19/1998

tions is best demonstrated by the isolation and characterization of a series of one- and two-dimensional solids such as $(H_3NCH_2CH_2NH_3)[Mo_3O_{10}]$,[13a] $(2,2'\text{-bipy})_m[(MoO_3)_n]$ family (bipy = bipyridine),[13b] $(4,4'\text{-H}_2\text{bpy})[Mo_7O_{22}]$ (bpy = bipyridine),[13c] $(NH_4)_2[Mo_3O_{10}]$,[14] $[H_3N(CH_2)_6NH_3][Mo_4O_{13}]$,[15a] $Na(NH_4)[Mo_3O_{10}]$,[15a] and $(H_2\text{pip})[Mo_5O_{16}]$ (pip = piperizine).[15b] Examination of the crystallization conditions and crystal structures of these $Mo_xO_y^{n-}$ based hybrid phases reveals that the assembly process is controlled by the acidity of initial reaction mixtures and, more critically, by the choice of amines in consideration of size and charge to volume density matching the "desired" phases. Fusing the $Mo_xO_y^{n-}$ polyoxoanions by using simple amines, especially diamines (aliphatic and aromatic), has evolved a number of novel phases;[13−15] however, the applications of other organic templating agents remain largely unexplored. In the course of our investigation on the assembly of molybdenum(VI) polyoxoanion based solid materials, we have hydrothermally synthesized a series of novel one-, two-, and three-dimensional organically templated solids.[15] Extending this idea, we seek to explore the assembly of molybdenum polyoxoanion based phases by using nonconventional templates. Here, we report the synthesis and structural characterization of three novel solids: two-dimensional $(NH_4)_2[Mo_4O_{13}]$ **(1)** and one-dimensional $(CN_3H_6)(NH_4)[Mo_3O_{10}]$ **(2)** and $(NH_4)_2[(NH_3CH_2COO)Mo_4O_{13}]\cdot H_2O$ **(3)**, in which the $[(NH_3CH_2COO)_2Mo_8O_{26}]^{4-}$ unit contains $NH_3CH_2COO^-$ ligand. Compounds **1**−**3** are crystallized in the presence of 4-aminobenzoic acid, guanidinium carbonate, and aminoacetic acid, respectively.

Experimental Section

All preparations were conducted under hydrothermal autogenous pressure conditions in PTFE-lined stainless steel autoclave reactors (~22 mL). Starting materials included $MoO_3\cdot H_2O$ (Ajax), 4-aminobenzoic acid (Aldrich), guanidinium carbonate (Fluka), aminoacetic acid (AnalaR), and distilled H_2O (lab-made). Acidity of initial mixtures was adjusted using 37% HCl (aq) (Ajax) when necessary. All reagents were used as received without further purification. No hazards were encountered in the experimental work reported. All crystalline products were recovered by filtration and repeated washing with distilled H_2O. The CHN analysis was performed on a Leco CHNS-932 analyzer. Simultaneous TGA/DTA was performed on a Du Pont 9900 thermal analyzer from room temperature to 1000 °C in a N_2 stream at a flow rate of 10 °C min^{-1}. Powder XRD (PXRD) patterns were collected using a Siemens D5005 diffractometer with graphite-monochromated Cu Kα radiation ($\lambda = 1.5418$ Å) in the range of $3.5 < 2\theta < 60°$. High-temperature PXRD patterns were obtained by running samples in situ on the same instrument using a HTK16 attachment in the temperature range from room temperature to 1200 °C under a vacuum (~10^{-3} Torr).

Synthesis of $(NH_4)_2[Mo_4O_{13}]$ (1). A mixture of $MoO_3\cdot H_2O$ (1.13 g), 4-aminobenzoic acid (0.48 g), and H_2O (25 mL) in the mole ratio 1:0.5:200 was acidified to pH ≅ 4. The mixture was sealed in the autoclave reactor and heated at 120 °C for 168 h. The recovered solid products contained homogeneous white crystals. The CHN elemental analysis gave [observed (*calculated*)] C, 0 (*0.00*); N, 4.60 (*4.46*); H, 1.19 (*1.28*), which confirmed an empirical formula of $(NH_4)_2[Mo_4O_{13}]$ for **1**.

Synthesis of $(CN_3H_6)(NH_4)[Mo_3O_{10}]$ (2). A mixture of $MoO_3\cdot H_2O$ (1.13 g), guanidinium carbonate (0.32 g), and H_2O (25 mL) in the mole ratio 1:0.25:200 was acidified to pH ≅ 6. The white slurry of the mixture was sealed in the autoclave reactor and crystallization was completed after 120 h at 120 °C. The recovered white crystals of **2** were monophasic, as confirmed by the good match between the observed and calculated (using single-crystal X-ray diffraction data) powder X-ray diffraction patterns. Hydrothermal reaction of $MoO_3\cdot H_2O$, guanidinium carbonate, and H_2O in the mole ratio 1:0.5:200 at 120 °C for 120 h resulted in the crystallization of **2** and **2′** of distinct morphologies. The CHN elemental analysis of **2** and hand-picked crystals of **2′** gave [observed (*calculated*)] C, 2.38 (*2.28*); H, 2.01 (*1.92*); N, 10.70 (*10.66*) for **2** and C, 5.08 (*5.09*); H, 2.54 (*2.56*); N, 17.8 (*17.81*) for **2′**. These confirmed the empirical formulas of $(CN_3H_6)(NH_4)[Mo_3O_{10}]$ for **2** and $(CN_3H_6)_3[Mo_{3.5}O_{12}]$ for **2′**. [Crystal data for **2′**: $C_3H_{18}Mo_{3.5}N_9O_{12}$, $M_w = 708.05$, monoclinic space group *C*2/*c*, $a = 11.980(2)$ Å, $b = 15.953(3)$ Å, $c = 19.925(4)$ Å, $\beta = 92.29(3)°$, $V = 3805.2(13)$ Å^3, $Z = 8$, $D_{calc} = 2.472$ g cm^{-3}, $\mu = 2.336$ mm^{-1}, 2615 reflections, $R_1 = 0.0212$ [$I > 2\sigma(I)$]].

Synthesis of $(NH_4)_2[(NH_3CH_2COO)Mo_4O_{13}]\cdot H_2O$ (3). The reaction of $MoO_3\cdot H_2O$ (0.9 g), aminoacetic acid (0.42), and H_2O (25 mL) in the mole ratio 1:1:200 (pH adjusted to 4.5) at 120 °C for 168 h yielded homogeneous white crystals of **3**. The CHN elemental analysis gave [observed (*calculated*)] C, 3.32 (*3.33*); H, 1.99 (*2.10*); N, 5.86 (*5.83*), which confirmed an empirical formula of $(NH_4)_2[(NH_3CH_2COO)Mo_4O_{13}]\cdot H_2O$ for **3**.

DT/TG Analysis. Simultaneous DT/TG analysis was conducted on a NETZSCHSTA 409C thermal analyzer at a heating rate of 10 °C min^{-1} from room temperature to 1000 °C in an Ar/He atmosphere. The results are as follows.

$(NH_4)_2[Mo_4O_{13}]$, ***1.*** Two thermal changes occurred at 357 °C and between 400 and 520 °C with accompanying weight losses of 9.0 and 3.4%, respectively. The first endothermic change indicated the removal of NH_4^+ cations [NH_4/**1** = 5.7%] and partial structural fragmentation; the subsequent thermal change was attributed to further structural fragmentation as supported by the in situ XRD studies.

$(CN_3H_6)(NH_4)[Mo_3O_{10}]$, ***2.*** A broad endothermic change accompanied by a weight loss of 22.2% occurred in the temperature range 300−400 °C. This was attributed to the removal of NH_4^+ and $CN_3H_6^+$ cations [$(NH_4^+ + CN_3H_6^+)$/**2** = 14.8%] and accompanied phase transformation. *$(NH_4)_2[(NH_3CH_2COO)Mo_4O_{13}]\cdot H_2O$*, ***3.*** One broad endothermic change and one sharp exothermic change occurred between 180−340 and 400−450 °C with accompanying weight losses of 20.8% and 5.6%, respectively. These may be attributed to the removal of H_2O and NH_4^+ and the dissociation of $NH_3CH_2COO^-$ from the $[(NH_3CH_2COO)_2Mo_8O_{26}]^{4-}$ unit [$(NH_4^+ + H_2O + NH_3CH_2COO)$/**3** = 18.4%], which caused structural fragmentation.

X-ray Crystallographic Studies. The crystal structures of **1**−**3** were determined from the single-crystal X-ray diffraction data. The intensity data were collected by a $\theta/2\theta$ scan on a Siemens P4 X-ray diffractometer with graphite-monochromated Mo Kα radiation. Empirical absorption corrections were made from ψ-scan data using SHELXTL PC[16] at the data reduction stage along with the correction for Lorentz and polarization factors. Unit cell constants were determined from the positions of 20−25 centered reflections ($5.0° < 2\theta < 25.0°$) and optimized by the least-squares refinement. The systematic absence conditions of the reduced data together with the refinement results suggested the space group *Pbca* (No. 61) for **1**, $P2_1/c$ (No. 14) for **2**, and *C*2/*c* (No. 15) for **3**. All structures were solved by direct methods and refined by full-matrix least-squares on F^2 using the SHELXTL-PLUS package.[16] All non-hydrogen atoms were refined anisotropically. The positions of the hydrogen atoms of H_2O and NH_4^+ were found from difference maps, and those attached to carbon and nitrogen atoms of organic molecules were placed at calculated positions. All hydrogen atoms were refined isotropically using

(15) (a) Xu, Y.; An, L. H.; Koh, L. L. *Chem. Mater.* **1996**, *8*, 814. (b) Xu, Y.; Koh, L. L.; An, L. H.; Roshan, D. G.; Gan, L. H. *Studies on Surface Science and Catalysis;* Elsevier: Amsterdam, 1997; Vol. 105C, 2123. (c) Xu, Y.; Zhang, B.; Goh, N. K.; Chia, L. S. *Inorg. Chim. Acta* **1998**, in press. (d) Lu, J. J.; Xu, Y.; Goh, N. K.; Chia, L. S. *Chem. Commun.* **1998,** in press.

(16) Sheldrick, G. M. SHELXTL PC. Version 5.0. Siemens Analytical Instruments Inc., Madison, WI, 1994.

Table 1. Crystal Data and Refinement Details for (1)−(3)

	1	2	3
formula	$H_8Mo_4N_2O_{13}$	$CH_{10}Mo_3N_4O_{10}$	$C_2H_{15}Mo_4N_3O_{16}$
fw	627.84	525.95	720.93
color	white	white	white
crystal system	orthorhombic	monoclinic	monoclinic
space group	Pbca	$P2_1/c$	$C2/c$
a (Å)	7.682(5)	7.6158(13)	17.326(4)
b (Å)	15.389 (2)	16.5768(11)	10.744(2)
c (Å)	18.996(4)	9.1946(8)	18.697(4)
α (deg)	90	90	90
β (deg)	90	95.237(8)	108.27(3)
γ (deg)	90	90	90
V (Å^3)	2246(2)	1155.9(2)	3305.0(12)
Z	8	4	8
λ(Mo Kα) (Å)	0.71073	0.71073	0.71073
D_{calc} (g cm^{-3})	3.714	3.022	2.898
μ(Mo Kα) (mm^{-1})	4.441	3.260	3.053
crystal size (mm)	0.20 × 0.20 × 0.10	0.25 × 0.20 × 0.15	0.20 × 0.20 × 0.15
T (K)	296	296	296
θ min., max. (deg)	2.10, 26.00	2.40, 25.00	2.20, 25.00
hkl data limits	−1→9, −1→18, −1→22	−1→9, −1→19, −10→10	−1→20, −1→12, −22→21
abs corr/T_{min}, T_{max}	0.8453, 0.9977	0.8494, 0.9905	0.7980,0.9910
no. observed refl	1972	2020	2896
no. variables	184	163	228
Δ*ρ* min.,max (e Å^{-3})	−1.292, 1.031	−0.744, 1.650	−0.552, 0.926
R_1 [a] [$I > 2\sigma(I)$]	0.0344	0.0281	0.0250
wR_2 [b] [$I > 2\sigma(I)$]	0.0841	0.0704	0.0538
S [c] (GOF)	0.999	1.022	1.047

[a] $R_1 = \sum||F_o| - |F_c||/\sum F_o$. [b] $wR_2 = \{\sum[w(F_o^2 - F_c^2)^2]/\sum[w(F_o^2)^2]\}^{1/2}$. [c] $S = \{\sum[w(F_o^2 - F_c^2)^2]/(n - p)\}^{1/2}$.

Table 2. Atomic Positional Parameters [×10^4] and Equivalent Isotropic Displacement Parameters [Å × 10^3] for 1−3

	x	*y*	*z*	*U*(eq)		*x*	*y*	*z*	*U*(eq)
				Compound **1**					
Mo1	2091(1)	8596(1)	1011(1)	10(1)	O7	4301(7)	8314(3)	3056(3)	11(1)
Mo2	3296(1)	9292(1)	2563(1)	8(1)	O8	4430(7)	6551(3)	3223(3)	20(1)
Mo3	4227(1)	7204(1)	2511(1)	8(1)	O9	1355(7)	7275(3)	2820(3)	10(1)
Mo4	3853(1)	5661(1)	1102(1)	9(1)	O10	3285(7)	6442(3)	1828(3)	12(1)
O1	3854(8)	8741(4)	463(3)	22(1)	O11	5646(7)	6182(3)	771(3)	16(1)
O2	521(7)	9478(3)	776(3)	12(1)	O12	5755(7)	5130(3)	1958(3)	13(1)
O3	1049(7)	7706(3)	684(3)	18(1)	O13	2269(7)	5857(4)	487(3)	16(1)
O4	3114(7)	8199(3)	1855(3)	11(1)	N1	8744(12)	4213(5)	804(5)	20(2)
O5	2813(6)	9769(3)	1682(3)	10(1)	N2	2333(10)	7158(5)	−678(3)	22(2)
O6	1197(7)	9255(3)	2919(3)	14(1)					
				Compound **2**					
Mo1	−143(1)	5931(1)	9008(1)	12(1)	O7	2048(5)	4755(2)	6342(3)	24(1)
Mo2	2241(1)	4389(1)	8092(1)	12(1)	O8	4704(4)	4639(2)	8709(3)	15(1)
Mo3	4850(1)	5929(1)	9036(1)	12(1)	O9	4995(5)	6170(2)	7250(4)	26(1)
O1	241(5)	6896(2)	9598(4)	26(1)	O10	4476(4)	6827(2)	9876(4)	22(1)
O2	−705(5)	6025(2)	7172(4)	25(1)	N10	2842(6)	3025(3)	4822(4)	28(1)
O3	−16(4)	4572(2)	8778(3)	16(1)	N1	3266(7)	9446(3)	8756(5)	37(1)
O4	2325(4)	5650(2)	8955(3)	15(1)	N2	2992(8)	8169(3)	7840(5)	46(1)
O5	2345(4)	3354(2)	7850(3)	21(1)	N3	1683(6)	8512(3)	9893(5)	34(1)
O6	2605(4)	4174(2)	10528(3)	14(1)	C1	2617(6)	8723(3)	8820(5)	22(1)
				Compound **3**					
Mo1	483(1)	7656(1)	−368(1)	14(1)	O10	3271(2)	7368(3)	465(2)	13(1)
Mo2	1179(1)	5860(1)	1091(1)	14(1)	O11	4220(2)	5630(3)	460(2)	17(1)
Mo3	2461(1)	8071(1)	853(1)	12(1)	O12	2617(2)	5459(3)	−435(2)	19(1)
Mo4	3337(1)	5383(1)	870(1)	15(1)	O13	3882(2)	5533(4)	1794(2)	32(1)
O1	−352(2)	7971(3)	−89(2)	26(1)	O14	3118(2)	3823(3)	743(2)	28(1)
O2	82(2)	7243(3)	−1293(2)	23(1)	O15	1333(2)	6272(4)	3023(2)	28(1)
O3	718(2)	5959(3)	32(2)	17(1)	Ow	5633(2)	4578(4)	1466(2)	29(1)
O4	1366(2)	7841(3)	832(2)	14(1)	N10	0	5552(6)	−2500	29(2)
O5	364(2)	6208(4)	1385(2)	26(1)	N20	5000	3307(6)	2500	35(2)
O6	1302(2)	4287(3)	1194(2)	27(1)	N30	−1361(3)	6301(4)	417(2)	23(1)
O7	1989(2)	6276(4)	2162(4)	23(1)	N1	3427(3)	6796(4)	3114(2)	23(1)
O8	2335(2)	6093(3)	907(2)	15(1)	C1	2733(3)	6775(5)	3409(3)	24(1)
O9	2988(2)	8348(3)	1770(2)	23(1)	C2	1939(3)	6399(5)	2827(3)	20(1)

a riding model. Excursions of electron density on the final Fourier map were observed near Mo atoms in all three compounds [**1**, $\Delta\rho_{max} = 1.031$ and $\Delta\rho_{min} = -1.292$ e Å^{-3}; **2**, $\Delta\rho_{max} = 1.650$ and $\Delta\rho_{min} = -0.744$ e Å^{-3}; **3**, $\Delta\rho_{max} = 0.926$ and $\Delta\rho_{min} = -0.552$ e Å^{-3}]. A summary of crystal data and refinement details for **1**−**3** is provided in Table 1. Atomic positional parameters and equivalent isotropic temperature factors for **1**−**3** are given in Table 2. Selected bond lengths and angles for **1**−**3** are given in Table 3.

Results and Discussion

The crystallization processes of the $Mo_xO_y^{n-}$ based solids reported here are very sensitive to the pH value

Table 3. Selected Bond Lengths (Å) and Angles (deg) for 1−3

				Compound **1**			
Mo1−O3	1.703(5)	Mo3−O8	1.692(5)	O1−Mo1−O2	105.6(3)	O10−Mo3−O4	83.8(2)
Mo1−O1	1.723(6)	Mo3−O9[b]	1.755(5)	O1−Mo1−O4	103.2(3)	O7−Mo3−O4	72.7(2)
Mo1−O2	1.870(5)	Mo3−O10	1.892(5)	O2−Mo1−O4	134.9(2)	O9−Mo3−O9[b]	171.2(2)
Mo1−O4	1.887(5)	Mo3−O7	1.999(5)	O3−Mo1−O5	162.8(2)	O8−Mo3−O4	157.3(2)
Mo1−O5	2.278(5)	Mo3−O4	2.152(5)	O12[a]−Mo2−O5	105.1(2)		
		Mo3−O9	2.285(5)	O12[a]−Mo2−O7	99.0(2)	O11−Mo4−O10	99.0(2)
Mo2−O12[a]	1.739(5)	Mo4−O11	1.714(5)	O5−Mo2−O4	74.6(2)	O11−Mo4−O2[c]	96.9(2)
Mo2−O6	1.749(5)	Mo4−O13	1.714(5)	O7−Mo2−O4	73.8(3)	O10−Mo4−O5[c]	84.0(2)
Mo2−O5	1.866(5)	Mo4−O10	1.881(5)	O6−Mo2−O6[b]	176.8(3)	O2[c]−Mo4−O5[c]	73.8(2)
Mo2−O7	1.932(5)	Mo4−O2[c]	1.982(5)	O12[a]−Mo2−O4	158.7(2)	O13−Mo4−O12	168.9(2)
Mo2−O4	2.158(5)	Mo4−O5[c]	2.175(5)	O7−Mo3−O8	95.2(2)	O11−Mo4−O5[c]	162.5(2)
Mo2−O6[b]	2.410(5)	Mo4−O12	2.333(5)	O8−Mo3−O10	102.4(2)	O10−Mo4−O2[c]	150.7(2)
				Compound **2**			
Mo1−O1	1.706(3)	Mo2−O8	1.955(3)	O2−Mo1−O4	98.8(2)	O3−Mo2−O4	74.43(12)
Mo1−O2	1.708(3)	Mo2−O4	2.235(3)	O2−Mo1−O6[d]	93.7(2)	O7−Mo2−O6	168.21(14)
Mo1−O4	1.941(3)	Mo2−O6	2.260(3)	O4−Mo1−O3	73.13(12)	O5−Mo2−O4	166.29(13)
Mo1−O6[d]	1.968(3)	Mo3−O9	1.703(3)	O6[d]−Mo1−O3[d]	74.84(12)	O3−Mo2−O8	137.73(14)
Mo1−O3[d]	2.193(3)	Mo3−O10	1.714(3)	O1−Mo1−O3	162.7(2)	O10−Mo3−O6[e]	100.72(14)
Mo1−O3	2.265(3)	Mo3−O6[e]	1.950(3)	O2−Mo1−O3[d]	159.9(2)	O10−Mo3−O4	91.08(14)
Mo2−O7	1.713(3)	Mo3−O4	1.973(3)	O4−Mo1−O6[d]	158.18(14)	O6[e]−Mo3−O8	88.86(12)
Mo2−O5	1.733(3)	Mo3−O8	2.160(3)	O8−Mo2−O4	72.70(10)	O4−Mo3−O8	74.05(13)
Mo2−O3	1.908(3)	Mo3−O8[e]	2.274(3)	O5−Mo2−O3	104.7(2)	O9−Mo3−O8[e]	163.5(2)
				O5−Mo2−O8	101.1(2)	O10−Mo3−O8	156.10(14)
						O6[e]−Mo3−O4	159.13(14)
				Compound **3**			
Mo1−O2	1.708(3)	Mo3−O9	1.697(3)	O1−Mo1−O11[f]	96.5(2)	O12[f]−Mo3−O4	99.9(2)
Mo1−O1	1.718(4)	Mo3−O12[f]	1.747(3)	O1−Mo1−O3	99.2(2)	O12[f]−Mo3−O10	98.63(14)
Mo1−O11[f]	1.934(3)	Mo3−O4	1.902(3)	O11[f]−Mo1−O10$_f$	73.23(13)	O4−Mo3−O8	75.89(13)
Mo1−O3	1.965(3)	Mo3−O10	1.924(3)	O3−Mo1−O10[f]	85.92(13)	O10−Mo3−O8	74.05(12)
Mo1−O10[f]	2.224(3)	Mo3−O8	2.142(3)	O1−Mo1−O10[f]	163.5(2)	O9−Mo3−O10[f]	178.5(2)
Mo1−O4	2.295(3)	Mo3−O10[f]	2.437(3)	O2−Mo1−O4	161.39(14)	O12[f]−Mo3−O8	157.32(14)
Mo2−O6	1.706(4)	Mo4−O13	1.697(4)	O5−Mo2−O3	101.8(2)	O14−Mo4−O8	103.3(2)
Mo2−O5	1.710(3)	Mo4−O14	1.719(4)	O5−Mo2−O7	91.1(2)	O14−Mo4−O11	104.3(2)
Mo2−O3	1.891(3)	Mo4−O8	1.916(3)	O3−Mo2−O8	86.26(13)	O8−Mo4−O10	71.60(12)
Mo2−O7	2.102(3)	Mo4−O11	1.933(3)	O7−Mo2−O8	75.55(12)	O11−Mo4−O10	72.55(12)
Mo2−O8	2.151(3)	Mo4−O10	2.254(3)	O6−Mo2−O4	161.5(2)	O13−Mo4−O12	172.3(2)
Mo2−O4	2.228(3)	Mo4−O12	2.368(3)	O5−Mo2−O8	158.5(2)	O14−Mo4−O10	152.9(2)

[a] Symmetry transformations used to generate equivalent atoms: $-x+1, y+{}^1/_2, -z+1.2$. [b] $x+{}^1/_2, y, -z+{}^1/_2$. [c] $-x+{}^1/_2, y-{}^1/_2, z$. [d] $-x, -y+2$. [e] $-x+1, -y+1, -z+2$. [f] $-x+{}^1/_2, -y+{}^3/_2, -z$.

of the gel solution and the crystallization temperature. Some insight into the assembly of $Mo_xO_y^{n-}$ phases and the choice of templating agents can be gained by examining the assembly products and the type of templating molecules used. Amino acids contain both NH_2 and COO^- groups where the NH_2 group is expected to play a role as the templating agent and the COO^- group participates in the organization of $Mo_xO_y^{n-}$ to give cooperatively assembled organic/$Mo_xO_y^{n-}$ hybrid phases. However, 4-aminobenzoic acid is unstable under the crystallization conditions for **1**. Intensive investigation is undertaken to optimize the reaction conditions under which coorperative assembly of 4-aminobenzoic acid/$Mo_xO_y^{n-}$ can be achieved. In compound **(3)**, the aminoacetic group is attached to Mo atoms, as intended, through the carboxyl oxygen atom, forming $(NH_3CH_2COO)[Mo_xO_y]^{n-}$ clusters; however, further condensation of the $(NH_3CH_2COO)[Mo_xO_y]^{n-}$ cluster is hindered under the reaction conditions, and the cause of the effect is still under investigation.

One-dimensional chain structures appear to be one of the favorable networking patterns of oxomolybdenum polyhedra under hydrothermal conditions; examples include $(NH_4)_2[Mo_3O_{10}]$[14] and $Na(NH_4)[Mo_3O_{10}]$.[15] By simple extrapolation, a large cation, $CN_3H_6^+$, is introduced into the reaction mixture of $Mo_nO_y^{n-}$ and, thrillingly, a similar chain structured $(CN_3H_6)(NH_4)[Mo_3O_{10}]$ **(2)** is obtained where $CN_3H_6^+$ and NH_4^+ cations coexist in the interchain region. Increasing in the $CN_3H_6^+$ content in the reaction mixtures results in the crystallization of **2′** which consists of $Mo_7O_{24}^{6-}$ clusters charge-compensated and stabilized by $CN_3H_6^+$ cations.

The structure of $(NH_4)_2[Mo_4O_{13}]$ **(1)** is composed of puckered $Mo_4O_{13}^{2-}$ layers of corner- and edge-sharing MoO_6 octahedra and MoO_5 square pyramids in 3:1 ratio, as shown in Figure 1a. Each Mo receives distinct contributions, as shown in Figure 1a inset and Table 2: two terminal oxo groups, one 2-coordinated oxo group, and two 3-coordinated for Mo1; four 2-coordinated oxo groups and two 3-coordinated oxo groups for Mo2; one terminal oxo group, four 2-coordinated oxo groups, and one 3-coordinated oxo group for Mo3; and two terminal oxo groups, three 2-coordinated oxo groups, and one 3-coordinated oxo group for Mo4. The distinct feature of **1** lies in the coexistence of MoO_5 square pyramidal and MoO_6 octahedral units. The Mo−O bond lengths of MoO_5 are generally shorter than those of MoO_6. The puckered layers of $Mo_4O_{13}^{2-}$ are nearly parallel to the crystallographic *ab* plane. The layer structure of **1** can be described as being constructed from a Mo_4 tetrameric building unit containing three MoO_6 octahedra and one MoO_5 square pyramid connected through shared edges. Along the crystallographic *a* axis, the adjacent tetramers are joined by sharing two corners, forming chains. Along the crystallographic *b* axis, the tetramers are connected through the symmetry operation of the glide plane via shared corners into spirals (the highlighted area of Figure 1a). These spirals are packed in the

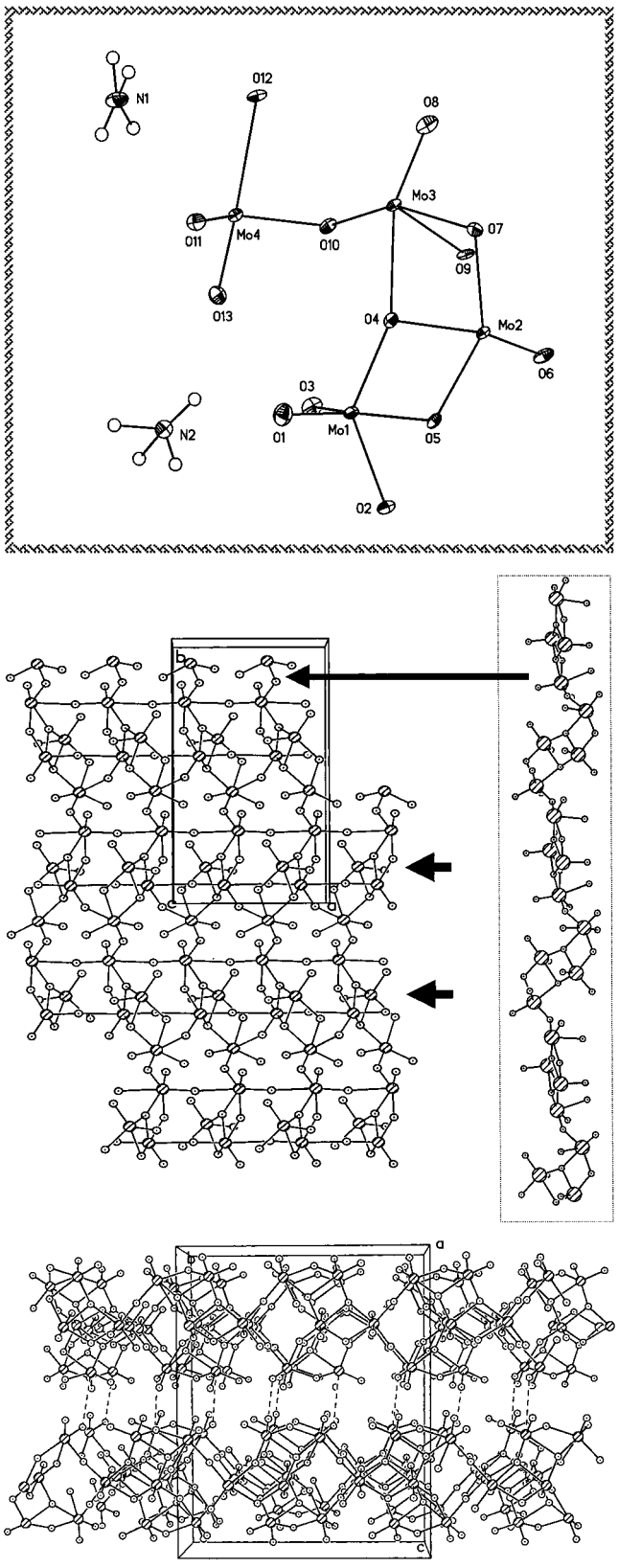

Figure 1. (a) The inset is the ORTEP view of the asymmetric unit of $(NH_4)_2[Mo_4O_{13}]$ **(1)** showing the atomic labeling scheme. The packing view of the $Mo_4O_{13}^{2-}$ layer of $(NH_4)_2[Mo_4O_{13}]$ **(1)** showing the connectivity of the tetrameric units along the crystallographic *ab* plane; highlighted is the connectivity of the tetramers along the *b*-axis. (b) The packing view of the $Mo_4O_{13}^{2-}$ layer of $(NH_4)_2[Mo_4O_{13}]$ (1) along the *a*-axis showing the interlayer separation, one-dimensional channels of 2- and 4-rings within the $Mo_4O_{13}^{2-}$ layer, and pseudo-one-dimensional channels of 4- and 6-rings in the interlamella region.

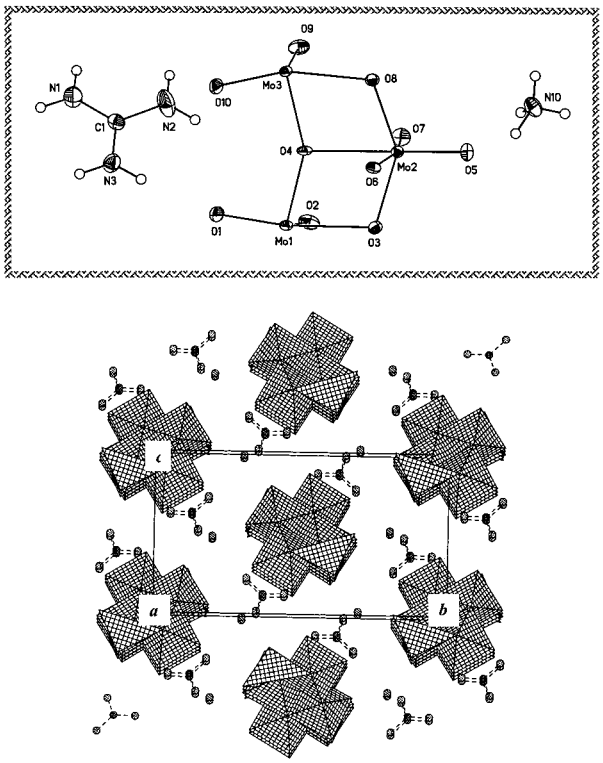

Figure 2. The packing view of the $Mo_3O_{10}^{2-}$ chains, $CN_3H_6^+$, and NH_4^+ of $(CN_3H_6)(NH_4)[Mo_3O_{10}]$ **(2)** along the *a*-axis. The inset is the ORTEP view of the asymmetric unit of **2** showing the atomic labeling scheme.

ABAB... order along the *ab* plane. This gives rise to one-dimensional 2- and 4-ring channels of the $Mo_4O_{13}^{2-}$ layers arranged in an alteration and running parallel to the crystallographic *a* axis, as shown in Figure 1b. The two-dimensional $Mo_4O_{13}^{2-}$ layer of **1** can be envisioned as being built up in space group *Pbca* from the aforementioned tetramers connected through shared corners.

The puckered $Mo_4O_{13}^{2-}$ layers of **1** are stacked along the crystallographic *c* axis with the interlamellar separation of 3.114(5) Å. The Mo−O···Mo contacts [Mo···Mo = 3.576(5) Å] are observed between adjacent layers which account for the formation of one-dimensional ***pseudo***channels of 4- and 6-rings. These pseudochannels are arranged in an alteration and run parallel to the crystallographic *a* axis. NH_4^+ cations occupy these pseudo-4- and -6-ring channels. Examination of the packing of **1** reveals the presence of hydrogen bonds of the type N(H)···O−Mo = 2.810(6)−3.302(7) Å, which bind the NH_4^+ cations tightly to the anionic layers of **1**. A similar layer structure for $Mo_4O_{13}^{2-}$ has also been found in a layered $BaMo_4O_{13}{\cdot}2H_2O$ which crystallizes in the space group *Pbna* (No. 60).[11c]

The structure of $(CN_3H_6)(NH_4)[Mo_3O_{10}]$ **(2)** consists of one-dimensional zigzag $Mo_3O_{10}^{2-}$ chains of corner- and edge-sharing MoO_6 octahedra. The coordination geometry of MoO_6 at each molybdenum site (Figure 2 inset) is defined by two terminal oxo groups and four unsymmetrical bridging oxo groups. Mo1, Mo2, and Mo3 show the typical two short−two intermediate−two long bond length pattern of molybdenunm(VI) oxides, as shown in Table 2. The parallel chains of $Mo_3O_{10}^{2-}$ are aligned along the crystallographic *a* axis and each chain has six immediate neighbors related by a pseudo-

6-fold axis, forming a cylindrical unit (Figure 2) similar to those of $(H_3NCH_2CH_2NH_3)[Mo_3O_{10}]$,[13a] $(NH_4)_2[Mo_3O_{10}]$,[14] $(H_3N(CH_2)_6NH_3)[Mo_4O_{13}]$, and $Na(NH_4)[Mo_3O_{10}]$.[15a] The adjacent chains are separated by a distance of 3.726(3) Å. This separation appears to be greater than those found in $(H_3N(CH_2)_6NH_3)[Mo_4O_{13}]$ [2.934(3) Å], $(H_3NCH_2CH_2NH_3)[Mo_3O_{10}]$ [3.070(1) Å], and $Na(NH_4)[Mo_3O_{10}]$ [3.084(5) Å]. We associate this with the size and packing arrangement of respective cations, which are $[H_3N(CH_2)_6NH_3]^+$ and $(H_3NCH_2CH_2NH_3)^+$, having nearly linear conformations and small Na^+ and NH_4^+, respectively.

In the structure of **2**, the $Mo_3O_{10}^{2-}$ chains are separated by large $CN_3H_6^+$ cations together with NH_4^+, where $CN_3H_6^+$ are planar and oriented nearly perpendicular to the running direction of the $Mo_3O_{10}^{2-}$ chains. The structure of **2** adopts such a packing arrangement that the electrostatic force between counterions is minimized as to stabilize the structure of **2**. Examination of the packing of **2** reveals significant H bonds of the types Mo−O···$CN_3H_6^+$ = 2.881(6)−2.935(7) Å and Mo−O···NH_4^+ = 2.796(7)−2.915(7) Å. The extensive hydrogen bonds contribute to stabilize the structure of $(CN_3H_6)(NH_4)[Mo_3O_{10}]$. Examination of the geometric parameters of the $CN_3H_6^+$ cations of **2** shows great similarity to those found in recently reported guanidinium−zinc−phosphates where complex H-bond networks exist.[17] It suggests a heavy involvement of $CN_3H_6^+$ cations through H-bonds in the stabilization of the structure of **2**.

The structure of $(NH_4)_2[(NH_3CH_2COO)Mo_4O_{13}]\cdot H_2O$ **(3)** consists of three-dimensional mixed covalent−hydrogen bonded $[(NH_3CH_2COO)_2Mo_8O_{26}]^{4-}$ clusters (Figure 3a) which are charge-compensated by NH_4^+ cations. The $[(NH_3CH_2COO)_2Mo_8O_{26}]^{4-}$ cluster is constructed from MoO_6 and $\{MoO_5(OOCCH_2NH_3)\}$ octahedral units, where the later receives contributions from terminal and bridging oxo groups as well as from aminoacetic groups. The Mo−O($OCCH_2NH_3$) bond [2.102(3) Å] is lengthened in comparison to other Mo−O bonds containing two-coordinated oxo groups [average, 1.973(3) Å] as shown in Table 2. Each anionic cluster of $[(NH_3CH_2COO)_2Mo_8O_{26}]^{4-}$ consists of two symmetry-related $[(NH_3CH_2COO)Mo_4O_{13}]^{2-}$ units, as shown in Figure 3b.

The packing of $[(NH_3CH_2COO)_2Mo_8O_{26}]^{4-}$, NH_4^+, and H_2O (Ow) is characterized by a complex network of weak interactions of the types MoO···Ow = 2.730(4)−2.905(3), MoO($OCCH_2H_3N$)···Ow = 2.876(4), MoO···NH_4^+ = 2.877(7)−2.957(6), NH_4^+···Ow = 2.860(7), and MoO($OCCH_2H_3N$)···OMo = 2.919(4)−2.959(3) Å. The hydrogen bonds formed between the neighboring $[(NH_3CH_2COO)_2Mo_8O_{26}]^{4-}$ clusters, as shown in Figure 3a, circumscribe large pseudo-one-dimensional channels in which NH_4^+ and H_2O are accommodated. The structure of **3** is stabilized by electrostatic forces as well as extensive nonbonding interactions.

Compounds **1** and **3** are synthesized using 4-aminobenzoic acid and aminoacetic acid as templating agents. The rational is to make use of the templating role of amino groups and the coordination capability of carboxyl groups to assemble novel molybdenum polyoxoanion based solids. During the crystallization of **1**, 4-aminobenzoic acid decomposes, forming NH_4^+ cations which serve to direct the assembly of molybdenum polyoxoanions. As a result, a novel layer structure consisting of $Mo_4O_{13}^{2-}$ is formed in which both MoO_6 octahedral and MoO_5 square pyramidal units coexist. In the crystallization of **3**, the aminoacetic acid survives and coordinates to Mo centers. It opens up the possibility of applying amino acids of various geometry and features for producing cooperatively assembled organic/molybdenum polyoxoanion solids with potentially interesting or useful properties.

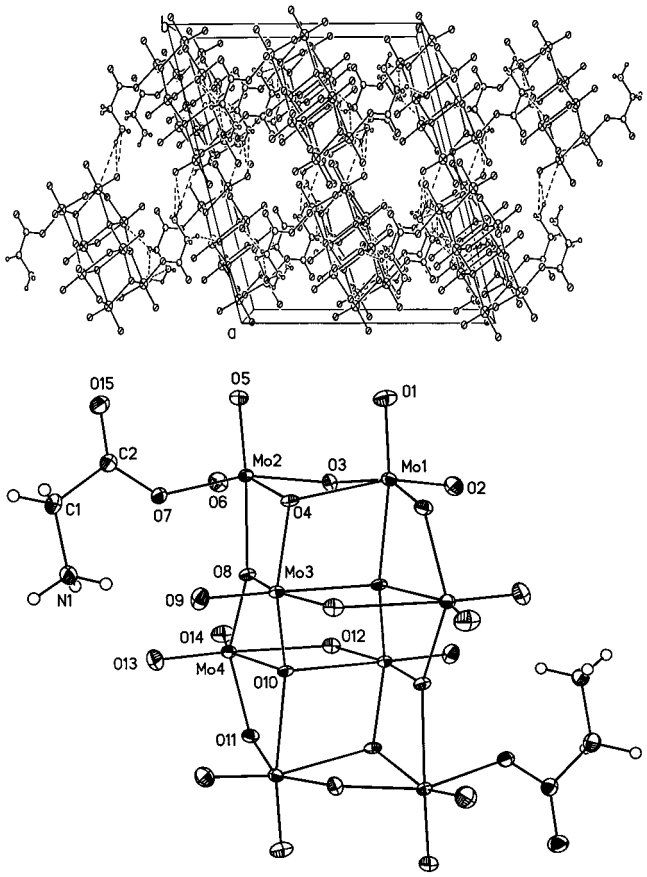

Figure 3. (a) The packing view of the $[(NH_3CH_2COO)_2Mo_8O_{26}]^{4-}$ cluster of $(NH_4)_2[(NH_3CH_2COO)Mo_4O_{13}]\cdot H_2O$ **(3)** along the *b*-axis showing the one-dimensional channels circumscribed by $[(NH_3CH_2COO)_2Mo_8O_{26}]^{4-}$ clusters through extensive H-bonds. (b) The ORTEP view of the $[(NH_3CH_2COO)Mo_4O_{13}]^{2-}$ cluster of $(NH_4)_2[(NH_3CH_2COO)Mo_4O_{13}]\cdot H_2O$ **(3)** showing the connectivity between carboxyl oxygen and Mo atoms and the atomic labeling scheme.

The structure of **2** is constructed from parallel chains of $Mo_3O_{10}^{2-}$ intercalated by $CN_3H_6^+$ and NH_4^+ cations through dominant electrostatic forces and moderate hydrogen bonds. The distinct feature of the $(CN_3H_6)(H_3O)[Mo_3O_{10}]$ phase lies on the successful incorporation of the nitrogen-rich guanidinium cations into the assembly of the $Mo_3O_{10}^{2-}$ chains. This represents the first attempt to explore the templating role of guanidinium ions in the assembly of molybdenum polyoxoanions. Experimental observation shows that the interstrand separation between the $Mo_3O_{10}^{2-}$ chains varies with the conformations and sizes of included cations. The successful isolation of **2** serves as a novel example of the retention of the coordination geometry of molecular building blocks in the preparation of new materials

(17) Harrison, W. T. A.; Phillips, M. L. F. *Chem. Mater.* **1997**, *9*, 1837.

through the combined effects of the hydrothermal technique and the structural templating agents.

Structural similarity between **1** and $BaMo_4O_{13}\cdot 2H_2O$,[11(c)] and between **2** and reported chain-structured oxomolybdenum polyhedra phases[13−15] provide further proof that a striking relationship could exist between the shape and charge to volume density of a template and the surrounding framework topology.[18]

Acknowledgment. We would like to thank the Nanyang Technological University (NTU) for financial support (RP 23/96XY). We are also grateful to the technical staff in the division of chemistry, School of Science, NTU for their supporting services.

(18) Lawton, S. L.; Rohrbaugh *Science* **1990**, *247*, 1319.

Supporting Information Available: Tables of experimental conditions and crystal data for X-ray diffraction structure determination, atomic positional parameters, bond lengths and angles, anisotropic temperature factors, and hydrogen atom positions for compounds **2** and **3** (11 pages); structure factors for **2** and **3** (12 pages). Ordering information is given on any current masthead page. A complete set of crystallographic data have been deposited at the Cambridge Crystallographic Data Centre (CCDC) for **1**−**3** and **2′**.

CM9805525